

Research Article

Solid Phase Extraction of Inorganic Mercury Using 5-Phenylazo-8-hydroxyquinoline and Determination by Cold Vapor Atomic Fluorescence Spectroscopy in Natural Water Samples

Mirna Daye,¹ Baghdad Ouddane,¹ Jalal Halwani,² and Mariam Hamzeh¹

¹ Université Lille 1, Equipe Chimie Analytique et Marine, UMR-CNRS 8217 Géosystèmes, Villeneuve d'Ascq Cedex, France

² Water & Environmental Sciences Laboratory (L.S.E.E), Lebanese University, Lebanon

Correspondence should be addressed to Baghdad Ouddane; baghdad.ouddane@univ-lille1.fr

Received 1 August 2013; Accepted 22 August 2013

Academic Editors: S. D'Ilio, T. Kaneta, S. Lee, and R. Zakrzewski

Copyright © 2013 Mirna Daye et al. This is an open access article distributed under the Creative Commons Attribution License, which permits unrestricted use, distribution, and reproduction in any medium, provided the original work is properly cited.

8-Hydroxyquinoline (8-HQ) was chosen as a powerful ligand for Hg solid phase extraction. Among several chelating resins based on 8-HQ, 5-phenylazo-8-hydroxyquinoline (5Ph8HQ) is used for mercury extraction in which the adsorption dynamics were fully studied. It has been shown that Hg(II) is totally absorbed by 5Ph8HQ within the first 30 minutes of contact time with $t_{1/2}$ 5 minutes, following Langmuir adsorption model. At pH 4, the affinity of mercury is unchallenged by other metals except, for Cu(II), which have shown higher K_d value. With these latter characteristics, 5Ph8HQ was examined for the preconcentration of trace levels of Hg(II). The developed method showed quantitative recoveries of Hg(II) with LOD = 0.21 $\mu\text{g mL}^{-1}$ and RSD = 3–6% using cold vapor atomic fluorescence spectroscopy (CV-AFS) with a preconcentration factor greater than 250.

1. Introduction

Mercury is a ubiquitous element and is one of the most toxic environmental pollutants. In aquatic environments, mercury exists mainly as three forms, which are elemental mercury (Hg^0), inorganic mercury Hg(II), and organic mercury. While all forms of mercury are poisonous, methyl mercury is the most toxic species due to its capacity of bioaccumulation through the aquatic food chain. The most employed analytical methods for trace mercury determination are inductively coupled plasma mass spectrometry (ICP-MS), Cold Vapor-Atomic Absorption Spectroscopy (CV-AAS), and cold vapor atomic fluorescence spectroscopy (CV-AFS). In natural waters, mercury concentration is found at trace levels in which most analytical techniques fail in its direct determination. Subsequently, a separation/preconcentration step is often indispensable. Among many preconcentration methods, solid phase extraction (SPE) is the most used for trace metal extraction.

8-Hydroxyquinoline (8-HQ) has a complexing coordinating ability with over 60 metals with preference to transition metals over alkali and alkaline earth metals. It is even used for the extraction of rare earth metals using a binary mixture of sec-octylphenoxyacetic acid-8-HQ [1]. 8-HQ forms chelates with metals of varying stability. $\log K_1$ values for Fe(III), Cu(II), Cd(II), Ca(II), and Mg(II) with 8-HQ are 13.7, 12.1, 7.3, 3.3, and 4.2, respectively [2]. Stability constant of Ca(II) with immobilized 8-HQ was also determined by [3] with slightly higher value of $\log K_1$ of 3.7. Moreover, Weaver and Harris [4] calculated the stability constant of aluminum with alkyl-immobilized 8-HQ and found it to be $\log K_1$ 0.8. High stability constants were found for Cd(II) with 8-HQ immobilized on controlled pore glass (CPG) ranging from 10^9 – 10^{11} [5]. 8-HQ has been used extensively for the preconcentration of trace metals from natural samples and seawater. Silica has been used as a support in many applications for its numerous advantages as compared to polymers. 8-HQ has been immobilized on various solid

matrices from XAD to activated carbon [6]. Adsorption capacities have been determined for some metals, that is, Cu(II) using 8-HQ functionalized CPG 58 $\mu\text{mole/g}$, Porasil C porous silica 104 $\mu\text{mole/g}$, and silica gel 216 $\mu\text{mole/g}$. It is evident that silica gel confers the largest capacity with an average molar coverage of 0.39 $\mu\text{mole/m}^2$ attributed to increased surface area of 553.84 m^2/g (decreased pore size) [7].

Numerous synthesis routes have been described since the first immobilization of 8-hydroxyquinoline (8-HQ) on silica gel. Diazo coupling of 8-HQ with p-aminobenzamide propyl silica was first reported in [23, 34]. The first techniques were further ameliorated by diazo coupling of 8-HQ on p-amino phenyl silica [24] or glass [25]. Moreover, the formation of Schiff's base on position 5 of 8-HQ moiety enables its fixation on p-aminopropyl silica bestowing extraordinary coordination [26]. Finally, following the Mannich reaction, which offers two possible procedures of 8-HQ immobilization on silica phase; one involving two steps reactions [27, 28] and the other one-step reaction [29, 30]. Among these synthesis routes, immobilization involving the diazo coupling of 8-HQ on p-aminobenzamide propyl silica was shown by many studies to have an excellent retention of many trace metals. The most powerful chelating 8-HQ-grafted silica is that with an exceptional coordination potential given by its anchoring position on carbon 5 of 8-HQ moiety. Therefore, phenylazo-8-HQ was chosen in this study among other 8-HQ-5-grafted silica due its higher yield product.

Since then much research has been conducted to fully understand the complexing ability of phenylazo-8-HQ (5Ph8HQ). Spectroscopic studies of metal complexes with 5Ph8HQ bound to silica showed 1:1 metal ligand stoichiometry in Cu^{2+} solution complex [31]. Other studies have determined the protonation constants of 5Ph8HQ-grafted silica to be $pK_{a1} = 2.7$ and $pK_{a2} = 8.6$ [31]. However, the water soluble sulfo-derivative of 8-HQ 5-(p-sulfophenylazo)-8-hydroxyquinoline showed higher acid dissociation constants, pK_{a1} of 3.78 and pK_{a2} of 7.94 [32]. These values would certainly change when the ligand is bound on silica. Equilibrium constants for 5Ph8HQ silica binding to metals have been determined. The stability constant of Cu^{2+} with the grafted material was $K^\circ = 4.8 \times 10^8$ [31], showing higher stability constant with Sulfo-5Ph8HQ in water, $K = 1.4 \times 10^{10}$ [32]. Recent study has showed higher equilibrium constant for Cu^{2+} than the previously reported ones for 5Ph8HQ in micelles and colloidal fumed silica-5Ph8HQ, $K^\circ = 1.27 \times 10^{11}$ and $K^\circ = 7 \times 10^{11}$, respectively [33]. Stability constant for Ni^{2+} was also determined and found to be $K^{\text{ext}} = 5.9$ [24] and $K^{\text{ext}} = 0.8\text{--}1.2$ for 1:1 ligand/metal stoichiometry in presence of either acetate or chloride counter ion [33]. Stability constants of metals with 8-HQ immobilized silica according to Luhrmann et al. [28] protocol were also determined, which involved the functionalization of p-aminopropyl silica with 5-chloro-methyl-8-hydroxyquinoline. Using Luhrmann protocol, distribution ratios $\log K_D$ were determined for many metals including Cu, Ni, Co, Fe, Mn, Cr, Zn, Cd, Hg, and Pb using batch equilibrium technique for 8-HQ-grafted silica. The use of the former protocol is not widely

studied because of its extremely high cost. Many studies have used 5Ph8HQ for the retention and preconcentration of metals with excellent recoveries [5, 34–38]. Nevertheless, the adsorption dynamics of 5Ph8HQ-grafted silica is not completely studied particularly for mercury. Thus, in this study we attempt to study the adsorption kinetics of mercury in single- and multielement solution to discover the competition demonstrated between mercury and different metals for 5Ph8HQ affinity sites. Moreover, in this study, adsorption isotherms of mercury and other metals were determined for 5Ph8HQ. Finally, an analytical method for the determination of Hg(II) in river water was developed based on 5Ph8HQ-linked silica as adsorbent and Cold Vapor Atomic Fluorescence Spectroscopy (CV-AFS) as an analytical instrument.

2. Materials and Methods

2.1. Chemicals and Materials

2.1.1. Reagents and Apparatus. Analytical reagent-grade chemicals were used and obtained Sigma Aldrich (France). Ultrapure water (with a resistivity of 18.2 $\text{M}\Omega$) was obtained using a Milli-Q system (Millipore, USA). Silica (100–200 mesh), chemicals, and solvents were supplied from Sigma Aldrich (France). Labware was soaked in 20% nitric acid and washed thoroughly with pure water prior to use. Working solutions of metals ions (Cr(III), Cu(II), Co(II), Zn(II), Ni(II), Pb(II), Cd(II), As(II), Fe(III), V(II), and Hg(II)) were prepared from stock metal nitrate solution (1000 mg/L) (Merck). Buffer solutions were prepared from 1 M sodium acetate to which different volumes of 1 M nitric acid were added to obtain pH in the range 4–6. Ammonium acetate and phosphate buffer were used for obtaining pH 7 and pH 8, respectively.

Fourier transform infrared (FT-IR) spectra of functionalized silica were recorded using Nicolet 380 Smart iTR spectrometer (ThermoScientific, USA) and were silica-matrix corrected. An inductively coupled plasma mass spectrometer, Thermo-Optek X7 (Thermo Fischer Scientific, USA), equipped with a cross-flow pneumatic nebulizer, a concentric glass-type nebulization chamber and a 1.5 mm i.d. quartz plasma torch, was used. All the operating parameters were those recommended by the manufacturer. The optimum operating conditions and measurement parameters for ICP-MS are listed in Table 1. Measurements were performed with high-purity Argon gas. The pH measurements and adjustments were conducted by pH meter (Thermo Scientific Orion Star A111, USA). The flow rates of the samples were adjusted using a Gilson Miniplus 3 peristaltic pump. PVC tubes (3.18 i.d) were used for the preconcentration process. Self-made PTFE (polytetrafluoroethylene) columns (65 mm \times 4 mm i.d.) were used for packing the examined adsorbent. Mercury was measured by cold vapor atomic fluorescence spectroscopy (Tekran, Model 2600 CVAFS Mercury Analysis System, USA). Ionic mercury is reduced with SnCl_2 (2% solution in 1% HCl), subsequently converted from Hg(II) to Hg° . The volatile species of mercury are separated from

TABLE 1: Operating conditions ICP-MS.

| | |
|--------------------------------|---|
| Forward power (W) | 1050 |
| Nebuliser gas flow (L/min) | 0,7 |
| Auxiliary gas flow (L/min) | 0,95 |
| Cool gas flow (L/min) | 13,5 |
| Quartz plasma torch I.D. (mm) | 1,5 |
| Cone type | Pt |
| Glass impact bead | 3 |
| Spray chamber temperature (°C) | |
| Nebulizer type | Glass concentric |
| Sample uptake rate (mL/min) | 1 |
| Uptake delay (s) | 35 |
| Washout delay (s) | 75 |
| Analytes | ⁵¹ V, ⁵² Cr, ⁵⁵ Mn, ⁵⁹ Co, ⁶⁰ Ni, ⁶⁵ Cu, ⁶⁶ Zn, ¹¹¹ Cd, ²⁰⁸ Pb, ⁵⁶ Fe, ⁷⁵ As |

solution by purging with high-purity argon gas through a semipermeable dryer tube. Volatile mercury is then carried by argon gas and preconcentrated into a gold cell of the cold vapor atomic fluorescence spectrometer. After thermal desorption, the concentration of Hg is determined by atomic fluorescence spectrometry at 253.7 nm.

2.2. Synthesis of 5Ph8HQ-Linked Silica Gel. Phenylazo-8-hydroxyquinoline silica gel was prepared according to the procedure proposed by Sugawara et al. [34]. The procedure firstly consists in a coupling step between an arylamine moiety and aminopropyl silica gel (APSG) to permit further azo-linking of 8-hydroxyquinoline on position 5. APSG (10 g) was also acylated by treatment with *p*-nitrobenzoyl chloride (1 g) in chloroform (60 mL) in presence of triethylamine (2 mL). The nitro adduct was then reduced by sodium dithionite (5% w/v solution) to yield aminobenzoyl-APSG. Oxidation of the amino moiety with sodium nitrite afforded formation of the expected diazonium salt, which was rapidly filtered to be coupled with 8-HQ. Formation of the final adduct was characterized by the rapid development of a deep red color, prominent feature of the formation of the expected diazo-linkage. Presence of the anchored 8-hydroxyquinoline was further ensured by FT-IR analysis, which revealed absorption bands from 1636 to 1524 cm⁻¹ relative to the presence of amide and heteroaromatic bonds.

2.3. Adsorption Experiments. A series of metal sorption experiments were conducted to study the effect of pH, sorption kinetics, selectivity, adsorption capacities, and interferences of mercury and some other metals. Batch experiments were conducted using 1000 mL polyethylene (PE) bottles. The amount of adsorbent used was 1 g and the volume of ultrapure water was maintained at 200 mL. A certain concentration of metal ion was prepared by dilution of stock solution (1000 mg/L M⁺) and adjusted to the required pH using an adequate buffer system. The bottles were shaken at room temperature for a fixed period of time at constant speed

150 rpm. At the end of shaking time, the supernatant was separated from the solid phase by filtration using Millipore filters and analyzed by ICP-MS for metals, and mercury analysis was performed using CV-AFS. The experiments were conducted in duplicates and the average results were reported. This methodology was followed to identify the pH effect, optimize shaking time, and understand the competition between metals towards 5Ph8HQ sites and its effect on mercury adsorption efficiency.

Metal uptake or sorption capacity was calculated based on the difference of metal ion concentration before and after adsorption according to (1). The percentage of mercury sorption, distribution coefficient, selectivity coefficients, and half-life sorption [39] were calculated using (1)–(5), respectively, as follows:

$$\text{Sorption (\%)} = \frac{C_i - C_{eq}}{C_i} \times 100, \quad (1)$$

$$Q = \frac{(C_i - C_{eq})V}{m}, \quad (2)$$

$$K_d = \frac{Q}{C_{eq}}, \quad (3)$$

$$\alpha = \frac{K_d(\text{Hg(II)})}{K_d(X)}, \quad (4)$$

$$t^{1/2} = \frac{1}{K_2 Q_{eq}}. \quad (5)$$

Here, C_i (mg/L) is the initial concentration; C_{eq} (mg/L) is the equilibrium concentration in the solution; V (L) is the solution volume; m (g) is the amount of sorbent; Q (mg/g) represents the sorption capacity and Q_{eq} represents the sorption capacity at equilibrium; K_d is distribution coefficient; α is the selectivity coefficient for the binding of a specific metal in the presence of other competitive ions; X represents the metal ion species.

2.4. Kinetics Studies. A certain concentration of metal ion solution was prepared and adjusted to the optimized pH using buffer system. An accurately measured sorbent of 1 g was added. Different aliquots were sampled and filtered at different time intervals for 24 hours. Sorption dynamics were studied in mercury single metal solution and binary solutions of Hg(II)-Cu(II), Hg(II)-Co(II), Hg(II)-Ni(II), Hg(II)-V(II), and Hg(II)-Fe(III). Moreover, adsorption kinetics were performed in multielement mixture composed of Hg(II), Cr(II), Fe(III), V(II), As(II), Co(II), Cu(II), Ni(II), Cd(II), Pb(II), and Mn(II).

Sorption kinetics were analyzed using pseudo-first- and second-order rate equations and intraparticle diffusion model. Chemical reactions in homogenous systems are described as pseudo-first-order rate equation. The linearized form of the first-order rate equation by Lagergren [40] is given as follows:

$$\text{Log}(Q_{eq} - Q_t) = \text{log } Q_{eq} - \frac{K_1 t}{2,303}, \quad (6)$$

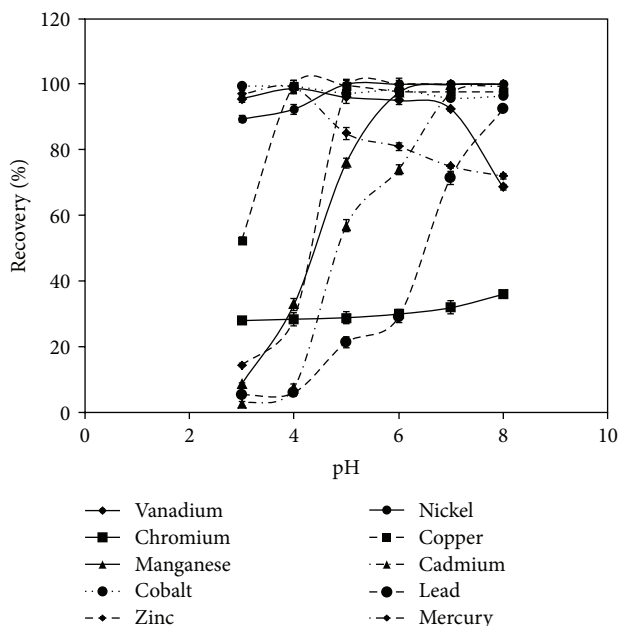


FIGURE 1: Effect of pH variation on the adsorption of metals. Conditions: volume: 200 mL, $m(5\text{Ph8HQ})$: 1 g, and $[M^+]$: $1 \mu\text{g mL}^{-1}$ in single-metal solution. Bars represent standard deviation for two replicates.

where Q_{eq} and Q_t are the amounts of metal ions adsorbed at equilibrium (mmol/g) and at contact t (min), respectively, and K_1 (1/min) is the rate constant.

The linearized equation of pseudosecond order rate equation was given by Ho and McKay [41] as follows:

$$\frac{1}{Q_t} = \frac{1}{K_2 Q_{\text{eq}}^2} + \left(\frac{1}{Q_{\text{eq}}} \right) t, \quad (7)$$

where K_2 (g/mmol·min) is the rate constant of pseudo-second-order adsorption reaction.

Intraparticle diffusion can be described to the model given by [42] by the following:

$$Q_t = K_i t^{1/2}, \quad (8)$$

where K_i is the intraparticle diffusion rate constant (mmol/g·min^{0.5}).

2.5. Adsorption Isotherms. Adsorption isotherms were determined for Hg(II). Accurately measured 1 g of the sorbent was mixed with 50 mL of solution adjusted to the Hg optimal pH. The concentration of metal ion was changed between 10–160 mg/L while being shaken (agitation speed 150 r/min). The contact time was selected on the basis of the kinetics studies. At equilibrium time, an aliquot was sampled, filtered, and analyzed. The results were adjusted to the Langmuir, Freundlich, and Dubinin-Radushkevich (D-R) models [43–45]. The Langmuir model linearized form is given by the following:

$$\frac{1}{Q_{\text{eq}}} = \frac{1}{Q_m} + \frac{1}{b Q_m C_{\text{eq}}}, \quad (9)$$

where Q_{eq} (mmole/g) is the amount of metal ion adsorbed, C_{eq} is the equilibrium metal ion concentration (mmol/L), Q_m (mmole/g) is the maximum Langmuir uptake when the surface of the adsorbent is completely covered with adsorbate, and b (L/mmole) is the Langmuir adsorption constant.

The Freundlich linearized form is described by (10):

$$\text{Log } Q_{\text{eq}} = \text{log } K_F + \frac{1}{n \text{log } C_{\text{eq}}}, \quad (10)$$

where Q_{eq} is the equilibrium metal ion concentration on the adsorbent (mmol/g), C_{eq} is the equilibrium concentration of metal ion (mmole/L), K_F is the Freundlich constant (mmole/g) which indicates the adsorption capacity and the strength of the adsorption, and n is the heterogeneity factor representing bond distribution.

The D-R adsorption isotherm linearized form is given by the following:

$$\ln Q = \ln Q_m - K \varepsilon^2, \quad (11)$$

where Q is the amount of metal ion adsorbed per unit weight of the sorbent (mole/g), K is a constant related to the adsorption energy ($\text{mol}^2/\text{KJ}^{-2}$), Q_m is the maximum adsorption capacity (mole/g), and ε is the Polanyi potential (J/mole).

2.6. Preconcentration Study. For optimization procedure, the synthesized 5Ph8HQ was cleaned by 20 mL of 2 M HNO_3 at flow rate 2 mL/min, washed by Milli-Q pure water until free from acid, and finally conditioned by acetate-acetic acid buffer system at flow rate 1 mL/min. Aliquots of 50 mL of river water containing of 2 ng mL^{-1} were adjusted to optimal extraction pH using ammonia or HNO_3 Suprapur solution. Samples were percolated through 300 mg precleaned resin at optimized flow rate, eluted with a suitable eluent, and finally analyzed by CV-AFS.

3. Results and Discussion

3.1. Effect of pH. The effect of pH variation on metal uptake of Hg(II), Cr(II), V(II), As(II), Co(II), Cu(II), Ni(II), Cd(II), Pb(II), Mn(II), and Zn(II) was investigated using batch procedure in single-metal solution. Solution acidity was varied between pH 3 and 8. At equilibrium time, aliquots were sampled, filtered, and analyzed. Metal ion sorption can occur through several single or mixed mechanisms. Coordination with the functional groups adhered to the sorbent through chelation, electrostatic attraction, and anion exchange with protonated amino group through proton or anion exchange.

Figure 1 shows the effect of pH variation on metal retention on the grafted material. The optimal adsorption of mercury was found in the range 3-4 with pH 4 as the optimal acidity. Above pH 4, Hg(II) retention decreases to 80% and follows a steady trend between pH 4 and 8. At pH greater than 5, mercury forms colloidal precipitate of $\text{Hg}(\text{OH})_2$ or soluble $\text{Hg}(\text{OH})^+$. The chemistry of mercury in aqueous solutions is more complicated than any other metal. Mercuric ions can be easily hydrolyzed according to the equation [46].

The coordination of water influences mercury adsorption dynamics and can relatively allow for slow diffusion,



The presence of Cl^- can result in the formation of HgCl^+ , HgCl_2 and HgCl_4^{2-} , HgCl_3^- [47] and in the possible electrostatic adsorption on the resin depending on its charged form. The increase in retention might be attributed to these species and not due to free $\text{Hg}(\text{II})$. Lower pH values are expected to enhance protonated ligand sites available for adsorption. Beyond pH 6, mercury uptake can decrease due to precipitation for high concentration, which is therefore not applicable in our case. The pH dependence of metal adsorption is the result of the effect of metal speciation and the ionization forms of different groups of the sorbent. The adsorption of mercury is possibly complexation and not chemical binding since the zeta potential of 5Ph8HQ is zero [33]. The affinity of mercury toward the donor set atoms of 5Ph8HQ is due to hard and soft acid base theory. It correlates the degree of metal softness to the observed strength of interaction with the donor atoms (N, O). Mercury is considered as a soft metal, because of its relatively large ionic size, low electronegativity, and high polarisability. The N=N, -NH, and OH of 5Ph8HQ are considered relatively soft bases leading to the observed high affinities between each other.

The stability constant of $\text{Cu}(\text{II})$ with 8-HQ is elevated ($\log \beta = 12.56$) [48], which is demonstrated by high distribution coefficient value as discussed below. Quantitative adsorption of $\text{Cu}(\text{II})$ is found for pH values greater than 4 and then slightly decreases due to the formation of strong complexes with carbonates $\text{Cu}(\text{CO}_3)_2^{2-}$ ($\log \beta = 10.69$) [49]. The retention of $\text{Cd}(\text{II})$ is shown to be low for $\text{pH} < 6$, in which Turner et al. [49] reported that 96% of Cd are found as ionic free species for $\text{pH} = 6$. In seawater, it has been reported that when $\text{pH} < 6$, Cd forms chlorocomplexes CdCl_2 , CdCl_3^- , and CdCl_4^{2-} with high stability constants $\log \beta = 2.59$, $\log \beta = 2.4$, and $\log \beta = 1.47$ [49], respectively, which impedes its complexation with 8-HQ. Thereby, quantitative retention is achieved for pH values > 6 , with the formation of weak hydroxide complexes $\text{Cd}(\text{OH})^+$, $\text{Cd}(\text{OH})_2$, and $\text{Cd}(\text{OH})_3^-$ of $\log \beta = -10.08$, $\log \beta = -20.35$, and $\log \beta = -33.3$ [49]. The stability constant of Cd with 8-HQ is high, $\log \beta = 7.78$, which can easily break down the weak complexes formed with hydroxides. As for $\text{Mn}(\text{II})$, quantitative retention is attained for pH values > 6 . At basic medium, Mn forms weak complexes with hydroxides $\text{Mn}(\text{OH})^+$ ($\log \beta = -10.59$), carbonates $\text{Mn}(\text{CO}_3)$ ($\log \beta = 4.1$) [49] which seems far from the competition with 8-HQ complexes ($\log \beta = 6.8$).

At acidic pH values, the stability constant of $\text{Ni}(\text{II})$ ($\log \beta = 9.27$) and H^+ ($\log \beta = 9.9$) with 8-HQ is comparable. Therefore, quantitative recoveries of $\text{Ni}(\text{II})$ are found for $\text{pH} \geq 5$ values although at pH 4 92.4% recovery of $\text{Ni}(\text{II})$ can be attained. As shown in Figure 1, the retention of $\text{Pb}(\text{II})$ at low pH values is almost negligible. This is due to the competition between $\text{Pb}(\text{II})$ and H^+ to form stable complexes with 8-HQ with $\log \beta = 9.1$ and $\log \beta = 9.9$, respectively. As have been described for $\text{Ni}(\text{II})$ and $\text{Pb}(\text{II})$, $\text{Zn}(\text{II})$ follows the

same behavior, with competition of H^+ ions at low pH values ($\log \beta = 9.9$) to form more stable complexes with 8-HQ than Zn -8-HQ complexes ($\log \beta = 8.56$). Therefore, quantitative retention of $\text{Zn}(\text{II})$ is observed for $\text{pH} \geq 5$.

Quantitative recovery of Vanadium is only seen for $3 < \text{pH} < 4$. At higher pH values, the retention decreases. This is explained by the formation of $\text{V}(\text{IV})$ species at pH values < 3.5 which are mainly VO^{2+} , $\text{VO}(\text{OH})^+$, $(\text{VO}(\text{OH}))_2^{2+}$, and $\text{VO}(\text{OH})_2$ [50]. At $3.5 < \text{pH} < 7.5$, anionic species form, mainly $\text{H}_2\text{VO}_4^{2-}$, and for $7.5 < \text{pH} < 13$, the anionic form of HVO_4^{2-} dominates [51]. The retention of $\text{Cr}(\text{III})$ at the studied pH range (3–8) is lower than 36%. It is probably due to the formation of chromium, under the oxidation state (V), which forms CrO_4^{2-} which certainly obstructs its complexation with 8-HQ [52].

Arsenic showed no adsorption by 5ph8HQ at the studied pH range (pH 3–8). In summary, the adsorption of $\text{Pb}(\text{II})$, $\text{Cd}(\text{II})$, and $\text{Mn}(\text{II})$ was almost negligible between pH 3 and 4, then it increased at $\text{pH} > 5$. It is shown that basic conditions are favorable for $\text{Pb}(\text{II})$ retention. At lower pH value, the retention of these metals drops off probably due to the partial protonation of active sites and the stronger electrostatic repulsion between $\text{Pb}(\text{II})$ and the protonated amino and hydroxyl groups of 5Ph8HQ. At basic medium, the retention is higher which is appreciated in selective separation from $\text{Hg}(\text{II})$, $\text{V}(\text{II})$, $\text{Cu}(\text{II})$, $\text{Ni}(\text{II})$, and $\text{Co}(\text{II})$. Moreover, at basic pH values, functional groups of the sorbent are free from protonation, and therefore, retention is controlled by chelation mechanism. The corresponding affinity of the resin is attributed to the protonation of the free lone pair of nitrogen suitable for coordination with metals. Values of pH higher than 8 were not examined to prevent hydrolysis of adsorbent and precipitation of metals. The optimal pH values for $\text{Hg}(\text{II})$ is 4, for $\text{V}(\text{II})$ is 4, for $\text{Cu}(\text{II})$ is 4, for $\text{Co}(\text{II})$ is 3–4, for $\text{Zn}(\text{II})$ and $\text{Ni}(\text{II})$ is 5–8, for $\text{Cd}(\text{II})$ and $\text{Pb}(\text{II})$ is 8, for $\text{Cr}(\text{II})$ is 7, for $\text{Mn}(\text{II})$ is 7–8. Therefore, at pH 4, simultaneous extractions $\text{Hg}(\text{II})$, $\text{V}(\text{II})$, $\text{Cu}(\text{II})$, $\text{Co}(\text{II})$, and $\text{Ni}(\text{II})$ can be achieved by 5Ph8HQ with maximal extractions occurring for $\text{Hg}(\text{II})$, $\text{V}(\text{IV})$, $\text{Cu}(\text{II})$, and $\text{Co}(\text{II})$ with prominent separation from $\text{Pb}(\text{II})$, $\text{Cd}(\text{II})$, $\text{Mn}(\text{II})$, and $\text{Zn}(\text{II})$.

3.2. Adsorption Dynamics. In order to determine the optimum contact time between 5Ph8HQ, adsorption recoveries (%) were measured as a function of time in single-metal solution and presented in Figure 2. Rapid uptake of metals by the resin was observed within the first 10 minutes. The time required to reach adsorption equilibrium was 30 minutes for $\text{V}(\text{IV})$, $\text{Cd}(\text{II})$, $\text{Cu}(\text{II})$, $\text{Zn}(\text{II})$, $\text{Hg}(\text{II})$, $\text{Ni}(\text{II})$, while slower equilibrium time was attained for $\text{Mn}(\text{II})$ 1 hour, and 5 hours for $\text{Co}(\text{II})$ and $\text{Pb}(\text{II})$. Adsorption time equilibrium was comparable to other resins, and in some cases, the adsorption is faster than others reported in the literature [53, 54]. On the other hand, in multielement mixture, equilibrium time of Hg and other metals has shifted to longer time, mainly because of interferences with other metals with stronger affinity to 5Ph8HQ. Mercury has reached equilibrium after 2 hours, while for $\text{Co}(\text{II})$, $\text{Ni}(\text{II})$, $\text{Zn}(\text{II})$, and $\text{Fe}(\text{III})$, the adsorption time was longer and did not reach quantitative recoveries

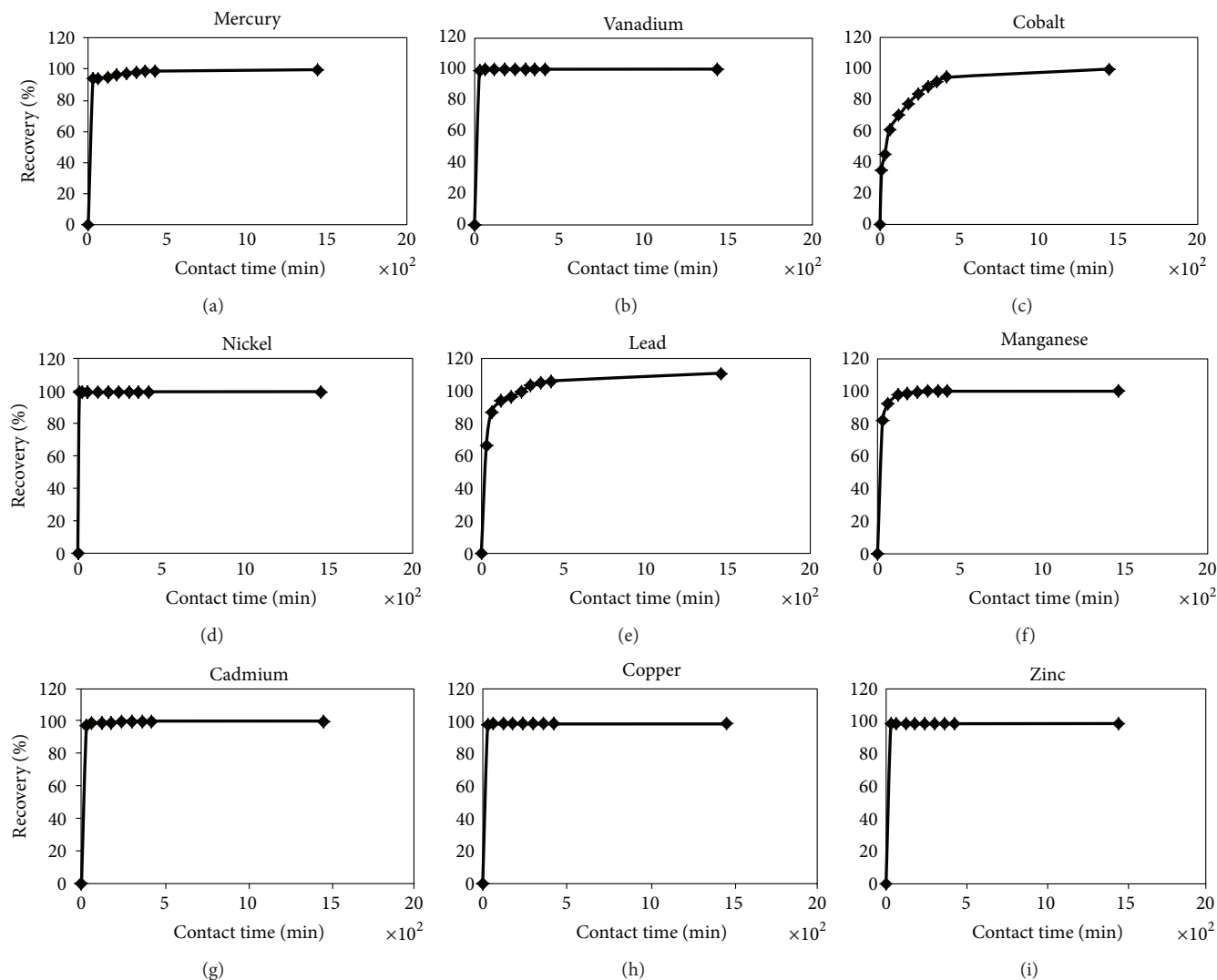


FIGURE 2: Recovery percentage of metals as function of time in a single-metal solution. Conditions: volume: 200 mL, $m(5\text{Ph}8\text{HQ})$: 1 g, element optimized pH, and $[M^+]$: $1 \mu\text{g mL}^{-1}$.

after 24 hour contact time. Still, the equilibrium time of Cu(II) and V(IV) has not been influenced in multielement mixture, revealing the significant affinity of these metals towards the studied resin.

In a single metal solution, the lowest half-life sorptions were that of Cu(II) 0.06 min < V(IV) 0.28 min < Ni(II) 0.39 min < Zn(II) 0.41 min < Cd(II) 0.89 min, respectively, while slower sorption kinetics were found for Hg(II) 5.39 min < Pb 25.23 min < Co(II) 49.96 min (Table 2). Overall, the fast adsorption of metals on 5Ph8HQ can be attributed to the good hydrophilicity of silica and the chelating strength of 5Ph8HQ towards metals. In order to interpret the sorption kinetics, Lagergren first-order equation, pseudo-second order equation, and Webber-Morris intraparticle diffusion models were used to evaluate the experimental data.

Table 2 shows adsorption kinetic parameters of different metals in single-metal solution. First-order rate K_1 was determined from the slope and intercept of the plot of

$\log(Q_{\text{eq}} - Q_t)$ versus t . The correlation coefficients (R^2) were between 0.99–0.79 for all studied metals and 0.9641 for Hg(II). As for pseudo second-order model, correlation coefficients were superior to 0.999 for all systems. The inapplicability of the first kinetic model suggests the prevalence of pseudo-second-order kinetic model on the adsorption of metals on the studied sorbent in which the calculated equilibrium adsorption capacities Q_e (theoretical) were in accordance with the experimental adsorption capacities Q_e (experimental). Thereby, chemisorption may control the adsorption mechanism involving valence forces through sharing or exchange of electrons between the resin and metals [55]. Moreover, the kinetic results were also fitted to intraparticle diffusion model by tracing q_t versus $t^{1/2}$. If the plots were straight lines passing through the origin, then the adsorption mechanism is governed by intraparticle diffusion defining the sole rate limiting step. If plot q_t versus $t^{1/2}$ did not pass the origin, then the adsorption might be

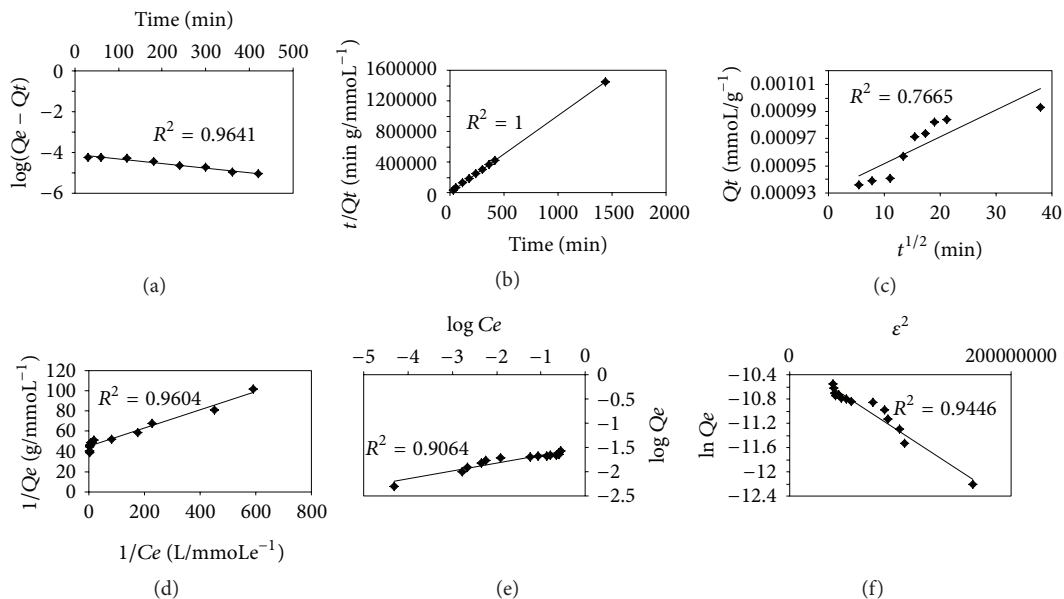


FIGURE 3: Adsorption kinetics of Hg(II) according to (a) pseudo-first-order model, (b) pseudo-second-order model, (c) intraparticle diffusion; [Hg²⁺]: 0.005 mmol L⁻¹, volume: 200 mL, pH: 4, and m(5Ph8HQ): 1 g. Adsorption isotherms of Hg(II) by 5Ph8HQ according to (d) Langmuir adsorption model, (e) Freundlich adsorption model, and (f) Dubinin-Radushkevich adsorption model; [Hg²⁺]: 10–160 μg mL⁻¹, volume: 50 mL, pH: 4, and m(5Ph8HQ): 1 g.

TABLE 2: Adsorption kinetics of metals in single-metal solution.

| Metal | First-order rate constants | | | | Second-order rate constant | | | Intraparticle diffusion | | |
|-------|--|--|-------------------------------------|----------------|--|--|----------------|-------------------------|----------------|----------------|
| | Q _e (exp) (mmol g ⁻¹) | Q _e (theor) (mmol g ⁻¹) | K ₁ (min ⁻¹) | R ² | Q _e (mmol g ⁻¹) | K ₂ (g mmol ⁻¹ min ⁻¹) | R ² | t ^{1/2} | K _i | R ² |
| Co | 0,003394 | 0,0020068 | 0,00576 | 0,9988 | 0,00326 | 6,140 | 0,9997 | 49,9 | 0,00005 | 0,7041 |
| V | 0,003926 | 0,0000176 | 0,00461 | 0,7997 | 0,00392 | 913,816 | 1 | 0,3 | 0,0000006 | 0,5295 |
| Pb | 0,000965 | 0,0003075 | 0,00530 | 0,9559 | 0,00091 | 43,728 | 0,9999 | 25,2 | 0,000009 | 0,6236 |
| Cd | 0,001779 | 0,0000601 | 0,01313 | 0,9368 | 0,00178 | 627,455 | 1 | 0,90 | 0,000001 | 0,5016 |
| Cu | 0,003152 | 0,0000044 | 0,00668 | 0,9478 | 0,00311 | 5116,770 | 1 | 0,06 | 0,0000001 | 0,5123 |
| Zn | 0,003059 | 0,0000122 | 0,00299 | 0,9195 | 0,00303 | 819,968 | 1 | 0,40 | 0,0000004 | 0,8384 |
| Mn | 0,003640 | 0,0010354 | 0,01958 | 0,9961 | 0,00365 | 83,622 | 1 | 3,27 | 0,00005 | 0,3805 |
| Ni | 0,003408 | 0,0000186 | 0,00484 | 0,9743 | 0,00340 | 739,984 | 1 | 0,40 | 0,0000005 | 0,7674 |
| Hg | 0,000997 | 0,0000789 | 0,00507 | 0,9641 | 0,00100 | 186,063 | 1 | 5,39 | 0,000002 | 0,7665 |

dominated by film diffusion or boundary layer diffusion [56]. As shown in Figure 3, the corresponding plot was not linear over the studied time range. Hg adsorption had an initial linear portion followed by a plateau suggesting the governance of intraparticle diffusion in the few hours of adsorption then film diffusion dominated. These two different stages of adsorption for Hg(II) are also seen for Co(II), V(IV), Cd(II), Cu(II), Zn(II), Ni(II), and Pb(II) with good correlation coefficients attained for Zn of 0.8 and Co, Ni, and Hg of 0.76. In contrast to other metals, Mn(II) demonstrated only film diffusion where a plateau is only seen.

In order to examine the influence of metals on the adsorption kinetics of mercury, adsorption kinetics were examined in multielement mixture. For this purpose, a certain metal

ion concentration containing V(IV), Cr(II), Co(II), Ni(II), Cu(II), Zn(II), Fe(III), and Hg(II) was added to 1 g of 5Ph8HQ at optimal pH for mercury sorption (pH 4). Metal mixture was shaken at 150 r.p.m and samples were taken at predetermined time as described above. As demonstrated in Table 3, the experimental data fitted-pseudo-second-order model with correlation coefficient between 0.9 and 1. The calculated equilibrium adsorption capacities for almost all metals tested were consistent with experimental data except for Co(II), Ni(II), and Zn(II). It seems that the adsorption of Ni, Co, and Zn is significantly affected in multielement mixture at pH 4. Similar to single-metal solution, film diffusion predominated the trend of adsorption of metals in multielement mixture except for Co which followed intraparticle diffusion model with correlation coefficients

of 0.97. Higher half-life sorption was found for all metals in multielement mixture, in which $t^{1/2}$ of some metals was tremendously affected. The $t^{1/2}$ of Ni(II) and Zn(II) were 230 and 61 higher in magnitude, respectively, than in single-metal solution. The sorption sequence of metals has been altered in multi-element solution with fast adsorption for Cu, V, and Hg. The $t^{1/2}$ sorption sequence became as follows: Cu(II) 0.7 min < V(IV) 1.86 min < Hg(II) 14.52 min < Zn(II) 25 min < Ni(II) 89.83 min < Fe(III) 124 min < Co(II) 119.61 min (Table 3). Therefore, in multi-element solution, Cu(II) and V(IV) appear to compete with Hg(II) for the adsorption sites of 5Ph8HQ since these metals have faster sorption times.

3.3. Competitive Adsorption

3.3.1. Multi-Element Mixture. The selectivity is determined by equilibrating a unit mass of the adsorbent in solution containing the same initial concentration for all metals. Solution acidity was adjusted to 4, which is the optimal pH for mercury adsorption. The overall adsorption efficiencies of Cu(II), V(IV), and Hg(II) remained unaffected in multi-component mixture. Maximum metal retention of 99.9%, 99.8%, 99.3%, 94.2%, 81%, 79%, 32.5%, 14%, and 10% were obtained for Cu(II), Hg(II), V(IV), Fe(III), Co(II), Ni(II), Zn(II), Pb(II), and Cd(II), respectively. As a result, the affinity order can be as follows: Cu(II) > Hg(II) > V(II) > Fe(III) > Ni(II) > Co(II) > Zn(II) > Pb(II) > Cd(II). The highest affinities (K_d) were obtained for Cu(II) 153.64, Hg(II) 50, and V(IV) 25 (Table 4). According to separation factor (α), mercury can be separated from metals of high affinity to 5Ph8HQ, that is, V(IV), Fe(III), Co(II), and Ni(II); however, Cu(II) poses a potential concurrence with Hg(II) towards the resin binding sites. This is ascribed to the higher distribution coefficient K_d Cu(II) 145.48 > K_d Hg(II) 50 and $\alpha < 1$.

3.3.2. Binary and Single Metal-Solution. Following the results of multi-element mixture, the highest affinities of metals towards 5Ph8HQ are obtained with an order: Cu(II) > Hg(II) > V(IV) > Fe(III) > Ni(II) > Co(II). Therefore, it is interesting to identify the effects of these metal ions with mercury in binary metal mixture at pH 4. The outlined order of metal ion selectivity by 5Ph8HQ based on the values of distribution coefficient and separation factor α is Cu(II) > Hg(II) > Co(II) > V(IV) > Ni(II) > Fe(III) (Table 5). It seems that the affinity order as seen in Table 4 has changed in binary metal mixture as compared to multi-element mixture with increased values of K_d and a decrease in the separation factor $\alpha_{\text{Hg}/\text{Mm}+}$. Change in the affinity of metals towards different sorbents with varying the competition potential was also observed in previous adsorption studies [57, 58]. According to the Irving-Williams series, the stability of metal complexes with ligands is in the order: Mn(II) < Fe(II) < Co(II) < Ni(II) < Cu(II) > Zn(II) [59]. The crystal field theory suggests electrostatic interaction between the central atom and the ligand. Therefore, there is a direct relationship between stability of metal complexes and ionic potential that is the charge to radius ratio (Z/r). Following the Z/r ratio cited in Table 6 of the studied metals, the selectivity sequence

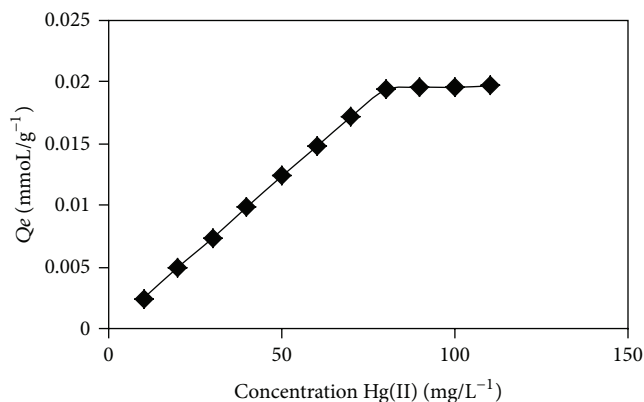


FIGURE 4: Adsorption profile of Hg(II) as a function of increasing metal concentration. Conditions: $[\text{Hg}^{2+}]$: 10–160 $\mu\text{g mL}^{-1}$, volume: 50 mL, pH: 4, and $m(5\text{Ph8HQ})$: 1 g.

is expected to be Mn(II) > Ni(II) > Co(II) = Zn(II) > V(II) > Cd(II) > Hg(II) and for trivalent metals As(III) > Cr(III) > Fe(III). The stability sequence of metals is not consistent with our results in either of the two mixed metal studies. The adsorption selectivity can shift from the predicted affinities depending on the experimental conditions (pH etc.) and sorbent properties. A direct correlation is made between Z/r ratio of metals and the metal complex stability in pure cation-exchange mechanism [60] that could be not ascribed to the studied resin. Therefore, it is also important to define the selectivity and the stability constants in single-metal solution without the presence of competitor elements.

Distribution coefficients are determined in single-metal solution at element-optimized pH. As demonstrated by Table 7, K_d has tremendously been altered to high values as opposed to that observed in multi-element mixture; still, K_d values for Cu(IV), V(II), and Hg(II) remained unchanged. Therefore, according to K_d values, metal affinity order towards 5Ph8HQ can be as follows: Mn(II) 999.8 > Co(II) 799.8 > Cd(II) 199.8 > Cu(II) 160 > V(IV) 137.73 > Ni(II) 59.5 > Hg(II) 52.37 > Zn(II) 18.84 > Pb(II) 2.4.

3.4. Adsorption Isotherms. Adsorption isotherm studies are of great value for their importance in describing the interaction between the solute, adsorbent, and the adsorbate. Thereby, the effect of initial concentration of metal sorption was investigated by varying the initial concentrations of metal ions at optimum pH. The obtained results were presented in Figure 3. As indicated in Figure 4, as the concentration of metal ion increases, the larger is the equilibrium adsorption uptake by the adsorbent. There seems to be a direct relation between the loading capacity of the sorbent and the metal ion concentration. It can be explained by the fact that, with higher concentration, the transfer driving force is larger [61]. The adsorption data for metals were analyzed and fitted according to Langmuir, Freundlich, and Dubinin-Radushkevich (D-R) models. The Langmuir isotherm model suggests monolayer sorption at specific homogenous site without interaction

TABLE 3: Adsorption kinetics of metals in multielement mixture at pH = 4.

| Metal | First-order rate constants | | | Second-order rate constant | | | | Intraparticle diffusion | |
|-------|---------------------------------------|-------------------------------------|----------------|-------------------------------|---|----------------|------------------|-------------------------|----------------|
| | Qe (theor) (mmol g ⁻¹) | K ₁ (min ⁻¹) | R ² | Qe (mmol/g ⁻¹) | K ₂ (g mmol ⁻¹ min ⁻¹) | R ² | t ^{1/2} | K _i | R ² |
| Co | 0,00146 | 0,00230 | 0,9533 | 0,00255 | 3,283 | 0,991 | 119,61 | 0,00004 | 0,9427 |
| V | 0,00007 | 0,00299 | 0,8843 | 0,00390 | 137,896 | 1 | 1,86 | 0,000003 | 0,4423 |
| Cu | 0,00004 | 0,00484 | 0,8318 | 0,00315 | 420,290 | 1 | 0,76 | 0,000001 | 0,6093 |
| Zn | 0,00033 | 0,00553 | 0,9541 | 0,00096 | 41,447 | 0,9998 | 25,04 | 0,000009 | 0,6659 |
| Ni | 0,00161 | 0,00345 | 0,9552 | 0,00267 | 4,169 | 0,9987 | 89,83 | 0,00004 | 0,7309 |
| Fe | 0,00193 | 0,00161 | 0,7571 | 0,00350 | 2,302 | 0,9993 | 124,09 | 0,000008 | 0,3698 |
| Hg | 0,00024 | 0,00668 | 0,7452 | 0,00100 | 68,596 | 0,9998 | 14,52 | 0,000009 | 0,4446 |

TABLE 4: Metal distribution coefficient (K_d) and separation factor (α) at pH 4 in multielement mixture.

| Element | V | Co | Ni | Cu | Zn | Cd | Pb | Fe | Hg |
|--|-------|--------|-------|--------|--------|---------|---------|-------|-------|
| K _d | 25.12 | 0.48 | 0.58 | 153.65 | 0.05 | 0.02 | 0.03 | 3.26 | 49.76 |
| α: K _d Hg/K _d M ⁺ | 1.98 | 102.87 | 85.99 | 0.32 | 931.16 | 2638.32 | 1468.79 | 15.28 | — |

between the sorbed molecules, with sites having identical adsorption energies. The Freundlich isotherm sorption assumes a monolayer sorption on heterogeneous sites with interaction between the adsorbent and that the adsorbate and all adsorption sites are energetically different. The D-R isotherm is considered more general than Langmuir model; it does not assume homogenous surface or constant adsorption potential. It is used to identify whether the adsorption is of a chemical nature or a physical one [44].

The model constants of Langmuir, Freundlich, and D-R isotherms along with correlation coefficients values are listed in Table 8. The R² values indicate that Langmuir fit the experimental data better than Freundlich and D-R isotherm models, suggesting a monolayer coverage of Hg(II) on 5Ph8HQ resin. Langmuir isotherm adsorption type was also found for Hg(II) with other studied resins, thiourea-modified chitosan [62] and poly-allyl thiourea [13]. The maximum adsorption capacity of Hg(II) on 5ph8HQ was found to be 0.022 mmole Hg(II)/g corresponding to a maximum Hg(II) initial concentration of 90 mg/L (Figure 4). The determined adsorption capacity is considered as minimal as compared to other resins such as thiol-functionalized mesoporous silica magnetite nanoparticles with 0.8 mmole Hg(II)/g [63] and 0.39 mmole Hg(II)/g of silica supported dithiocarbamate [64], 1.13 mmole Hg(II)/g of poly-allyl thiourea [13]. 8-Hydroxyquinoline silica synthesized according to Lührmann et al. [28] showed higher capacity for Hg(II) 0.448 mmole/g at optimized pH 6. The adsorption capacity for some metals has also been reported using HQ-silica synthesized according to different protocols. Marshall and Mottola [7] found an adsorption capacity for Cu(II) 0.227 mmole/g, while HQ-silica synthesized according to Pyell and Stork [27] showed higher capacity of 0.414 mmole/g and 0.248 mmole/g for Ni(II) and 0.333 mmole/g for Zn(II).

For Langmuir model, to determine if the resin is favorable for Hg(II) sorption, a dimensionless separation factor is defined as:

$$R_L = \frac{1}{1 + K_L C_i} \quad (13)$$

where K_L (L/mmole) is the Langmuir equilibrium constant and C_o (mmole/L) is the initial concentration of metal ion. If R_L > 1, the isotherm is unfavorable; if R_L = 1, the isotherm is linear; if 0 < R_L < 1, the isotherm is favorable; if R_L = 0 the isotherm is irreversible [65]. The value of R_L in this study was found to be 0.01, confirming the suitability of the resins for the recovery of Hg(II) ions. Moreover, the low R_L value < 0.1 implies strong interaction between Hg(II) and 5Ph8HQ.

3.5. 5Ph8HQ Column Extraction of Hg(II)

3.5.1. Flow Rate Optimization. The flow rate of Hg(II) solution through the column is an important parameter, in order to ensure sufficient contact time between the sorbent and the adsorbate and to control time of analysis. The flow rate of samples was investigated in the range between 1 and 5 mL/min. As shown in Figure 5, quantitative recoveries were obtained for flow rates between 2 and 3 mL/min. At flow rate > 3 mL/min, recoveries drop off to 93%. Therefore, a flow rate of 2 mL/min was used for the subsequent Hg(II) preconcentration.

3.5.2. Eluent Type and Volume Optimization. Elution of Hg(II) from 5Ph8HQ column was investigated by using different types of eluents, following the general procedure. The results demonstrated in Figure 6 showed that even with a mixture of HCl + HNO₃, Hg(II) ions have not been completely desorbed. However, the use HCl + HNO₃ as an eluent for metals from 5Ph8HQ was proven to be efficient [36, 37, 66]. This further accentuates the strong affinity of Hg(II) ions towards binding donor atoms (N, O) of 5Ph8HQ. In this case, as other studies have reported for the desorption of Hg(II) [13, 20], a strong complexing agent for mercury such as thiourea is added to varying concentrations of HCl. The obtained results show that 1 M HCl mixed with [CS(NH₂)₂] ≥ 2% was shown to be sufficient for quantitative desorption of Hg(II) ions (Figure 6). Even though 1 M HCl + 2% CS(NH₂)₂ was enough for the elution of Hg(II) ions, a larger elution volume of 10 mL was required for stripping off all the target

TABLE 5: Selectivity of mercury at pH 4 in binary mixtures.

| | V | Cu | Ni | Co | Fe | Hg |
|--------------------------------------|--------|---------|--------|--------|-------|--------|
| K_d | 27.011 | 159.800 | 12.829 | 35.836 | 5.260 | 52.376 |
| $\alpha: K_d\text{Hg}/K_d\text{M}^+$ | 1.939 | 0.3278 | 4.0825 | 1.462 | 9.957 | — |

TABLE 6: Metal ion charge to radius ratio [8].

| Ion | Oxidation state | Coordination number | Z/R |
|-----|-----------------|---------------------|-------|
| Pb | 2 | 6 | 1,68 |
| Zn | 2 | 6 | 2,7 |
| Cd | 2 | 6 | 2,11 |
| Cu | 2 | 6 | 2,74 |
| Ni | 2 | 6 | 2,9 |
| Cr | 3 | 6 | 4,88 |
| Co | 2 | 6 | 2,7 |
| V | 2 | 6 | 2,53 |
| Fe | 3 | 6 | 4,651 |
| Hg | 2 | 6 | 1,96 |
| As | 3 | 6 | 5,117 |
| Mn | 2 | 6 | 2,98 |

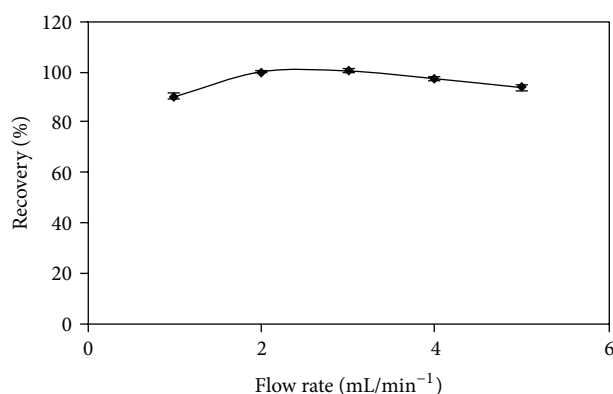


FIGURE 5: Effect of flow rate mercury by 5Ph8HQ column extraction. Conditions: $[\text{Hg}^{2+}]$: 2 ng mL^{-1} , V (50 mL), pH 4, and eluent: 5 M HCl + 5% $\text{CS}(\text{NH}_2)_2/10 \text{ mL}$. Bars represent standard deviation for two replicates.

ions. In order to achieve higher enrichment factor, 4 mL of 5 M HCl + 5% $\text{CS}(\text{NH}_2)_2$ was used for complete desorption at an optimized eluent flow rate of 0.5 mL/min (Figure 7).

3.5.3. Interferences. As shown in mercury adsorption dynamics section, the coexistence of equimolar metals with $\text{Hg}(\text{II})$ can prolong the equilibrium time due to the competition between mercury and other metals towards the relevant binding sites. Therefore, the effect of common interfering ions on the adsorption of $\text{Hg}(\text{II})$ was examined using batch experiment. For that purpose, 1g of the studied resin was equilibrated at pH 4 with 1 mg/L of $\text{Hg}(\text{II})$ and a certain concentration of the interfering ion. The mixture was shaken at 150 r.p.m and aliquots were taken at Hg equilibrium time and analyzed using CV-AFS. Results of Table 9 showed

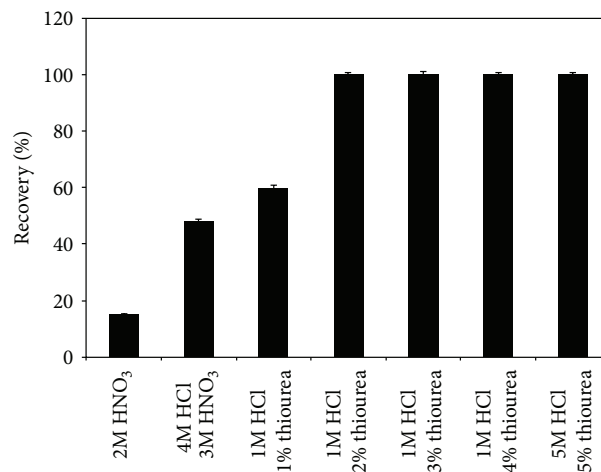


FIGURE 6: Elution recovery of $\text{Hg}(\text{II})$ adsorbed on 5Ph8HQ by column method using different types of eluents. Conditions: $[\text{Hg}^{2+}]$: 2 ng mL^{-1} , volume: 50 mL, pH: 4, and eluent volume: 10 mL. Bars represent standard deviation for two replicates.

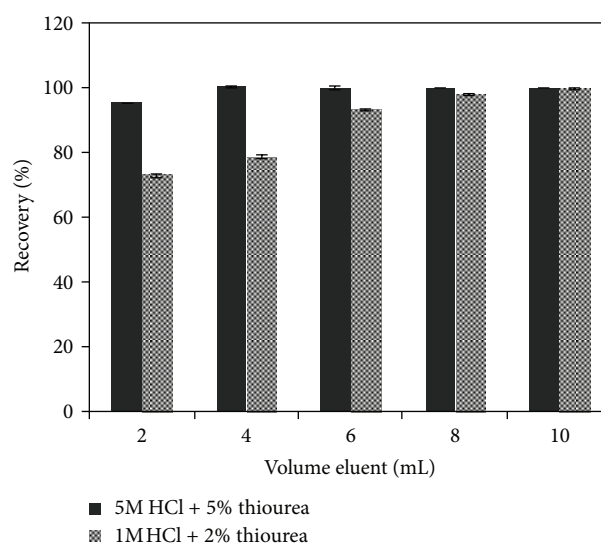


FIGURE 7: Effect of eluent volume on the recovery of $\text{Hg}(\text{II})$ adsorbed on 5Ph8HQ by column method. Conditions: $[\text{Hg}^{2+}]$: 2 ng mL^{-1} , V (50 mL), pH 4, and eluent: 5 M HCl + 5% $\text{CS}(\text{NH}_2)_2/1 \text{ M HCl} + 2\% \text{CS}(\text{NH}_2)_2$. Bars represent standard deviation for two replicates.

that several thousand fold excess of $\text{KNaC}_4\text{H}_4\text{O}_6$, Na_2CO_3 , $\text{Na}_3\text{C}_6\text{H}_5\text{O}_7$, humic acid had minor effect on the extraction of $\text{Hg}(\text{II})$ ions in which quantitative recoveries are still attained. Similarly, 10–100-fold excess of anions and major competing metals did not impose significant interferences, yet 4000-fold excess of $\text{Na}_2\text{C}_2\text{O}_4$ and KCN have decreased

TABLE 7: Distribution coefficients of metals in single-metal solution at element-optimized pH.

| Element | V | Co | Ni | Cu | Zn | Cd | Pb | Mn | Hg |
|---------|-------|-------|------|-------|------|-------|-----|-------|------|
| K_d | 137,7 | 799,8 | 59,5 | 160,6 | 18,8 | 199,8 | 2,4 | 999,8 | 52,3 |

TABLE 8: Langmuir, Freundlich, and D-R isotherm constants of Hg.

| Metal | Langmuir isotherms parameters | | | Freundlich isotherms parameters | | | D-R isotherms parameters | | |
|-------|-------------------------------|-----------------------------|--------|---------------------------------|--------|--------|------------------------------|--|--------|
| | Q_m (mmol g ⁻¹) | b (L mmol ⁻¹) | R^2 | K_F (mmol g ⁻¹) | n | R^2 | Q_m (mol g ⁻¹) | K (mol ² KJ ⁻²) | R^2 |
| Hg | 0,0224 | 492,815 | 0,9604 | 0,0311 | 6,1463 | 0,9064 | 0.000039 | 1×10^{-15} | 0,9446 |

TABLE 9: Effects of different electrolytes on the retention of Hg(II) ions.

| Electrolytes (cation/anion) | Foreign ion | Recovery (%) |
|---|-------------|--------------|
| Na ₂ CO ₃ ^a | 8,75 | 95,4 ± 0,15 |
| Na ₃ C ₆ H ₅ O ₇ ^a | 8,64 | 95,9 ± 0,16 |
| KNaC ₄ H ₄ O ₆ ^a | 20,76 | 96,7 ± 0,21 |
| Na ₂ C ₂ O ₄ ^a | 30,07 | 94,2 ± 0,11 |
| KCN ^a | 40,28 | 86,7 ± 0,22 |
| Humic acid ^b | 0,42 | 96,3 ± 0,14 |
| SO ₄ ^{2-a} | 1,04 | 97,0 ± 0,37 |
| Cl ^{-a} | 2,82 | 95,9 ± 0,26 |
| NO ₃ ^{-a} | 1,61 | 96,9 ± 0,22 |
| F ^{-a} | 0,53 | 94,5 ± 0,14 |
| Co ^{2+a} | 1,36 | 99,1 ± 0,11 |
| Fe ^{3+a} | 1,43 | 97,0 ± 0,91 |
| Ni ^{2+a} | 1,36 | 99,1 ± 0,23 |
| V ^{4+a} | 1,57 | 99,2 ± 0,15 |
| Cu ^{2+a} | 1,26 | 98,3 ± 0,85 |

a: mmol L⁻¹; b: g L⁻¹.

TABLE 10: Analytical results for the determination of Hg(II) in natural water samples by CV-AFS.

| Water samples | Concentration $\mu\text{g L}^{-1}$ | | Recovery (%) |
|---------------|------------------------------------|--------------------|--------------|
| | Added | Found ^a | |
| Tap water | 0 | 0,774 ± 0,034 | |
| | 0,5 | 1,274 ± 0,082 | 100 |
| | 2 | 2,769 ± 0,066 | 99,8 |
| River water | 0 | 0,382 ± 0,069 | |
| | 0,5 | 0,882 ± 0,085 | 100 |
| | 2 | 2,380 ± 0,055 | 99,9 |

^aThe value following "±" is the standard deviation ($n = 2$).

the Hg(II) retention to 94% and 87%, respectively. The latter high concentrations of 2–4 g/L are rarely seen in aquatic environments, which do not seem to impede the quantitative extraction of mercury from river water matrix.

3.5.4. Breakthrough Volume. It is determined by using the recommended column procedure as described above, using increasing volumes of Hg(II) solution while keeping the total amount of Hg(II) in the solution constant at 2 μg . Results have shown that the maximum sample volume can be up

to 2000 mL with the attainment of quantitative recovery and relative standard deviation <12%. The quantitative recovery of Hg(II) ions at high sample volumes is attributed to its high affinity and stability constant with 5Ph8HQ, in which most resins fail in Hg(II) extraction from large volumes [13]. Though a volume of 2000 mL was shown to extract effectively all target ions; a volume of 1000 mL was adopted for Hg(II) preconcentration in order to avoid long periods of extraction time ($t > 8$ hours). Considering 1000 mL as the sample volume and 4 mL as the eluent volume, an enrichment factor of 250 can be achieved.

3.5.5. Analytical Performance and Applications. The optimized method was applied for the extraction of trace levels of Hg(II) ions in tap and river water samples. A volume of 1000 mL was spiked with varying quantities of 2 μg and 0.5 μg of Hg(II). Results shown in Table 10 show that Hg(II) spikes were quantitatively extracted from both tap and river water. As shown in pH section of the adsorption dynamics, V(II), Cu(II), Ni(II), Co(II), and Zn(II) could be simultaneously extracted with Hg(II) ions at pH 4. Previous studies have reported a simultaneous extraction of metals at pH 6–8 [35–38, 67]. For this purpose, 1000 mL of tap water was spiked with 2 $\mu\text{g/L}$ of a multielement mixture containing V(II), Cu(II), Ni(II), Co(II), and Hg(II) and percolated at pH 4 through 300 mg 5Ph8HQ, eluted using 4 mL of 5 M HCl + 5% CS (NH₂)₂, and analyzed using ICP-MS for metals and CV-AFS for Hg(II) ions. Tables 10 and 11 demonstrate simultaneous quantitative extraction of V(II), Cu(II), Ni(II), Co(II), and Hg(II) at pH 4.

The detection limit was calculated according to IUPAC [68], which is three times the standard deviation (3 σ) of eight runs of blank solution and was 0.21 ng L⁻¹ for Hg(II) using CV-AFS. The detection limit of ICP-MS was also calculated for V(II), Co(II), Ni(II), and Cu(II) and found to be 0.28 ng L⁻¹, 0.4 ng L⁻¹, 1.5 ng L⁻¹, and 1.1 ng L⁻¹, respectively. The relative standard deviation (RSD) of 6 runs of 2 ng mL⁻¹ Hg(II) was lower than 6% indicating a good precision of the analytical method.

4. Conclusion

The optimized method was compared to previously developed analytical techniques for the measurements of trace levels of Hg(II). As can be seen from Table 12, the preconcentration factor is high in comparison to other methods.

TABLE 11: Simultaneous determination of metals in natural water samples by ICP-MS at pH 4.

| Water samples | Element | Concentration $\mu\text{g L}^{-1}$ | | Recovery (%) | |
|---------------|-------------|------------------------------------|--------------------|-------------------|------|
| | | Added | Found ^a | | |
| Tap water | V | 0 | 0,320 \pm 0,106 | 99,8 | |
| | | 2 | 2,315 \pm 0,21 | | |
| | Co | 0 | 0,059 \pm 0,004 | 99,1 | |
| | | 2 | 2,041 \pm 0,02 | | |
| | Ni | 0 | 4,392 \pm 0,037 | 96,5 | |
| | | 2 | 6,172 \pm 0,05 | | |
| | Cu | 0 | 0,762 \pm 0,137 | 99,9 | |
| | | 2 | 2,759 \pm 0,32 | | |
| | River water | V | 0 | 0,606 \pm 0,428 | 99,8 |
| | | | 2 | 2,602 \pm 0,52 | |
| Co | | 0 | 0,041 \pm 0,014 | 99,4 | |
| | | 2 | 2,030 \pm 0,05 | | |
| Ni | | 0 | 2,964 \pm 0,377 | 96,4 | |
| | | 2 | 4,790 \pm 0,52 | | |
| Cu | | 0 | 0,066 \pm 0,42 | 99,9 | |
| | | 2 | 2,065 \pm 0,32 | | |

^aThe value following “ \pm ” is the standard deviation ($n = 2$).

TABLE 12: Comparison of figures of merits for different preconcentration methods for Hg(II) ion.

| Chelating resin | DT ^a | pH | Capacity ($\text{mmol}\cdot\text{g}^{-1}$) | LOD ^b ($\text{pg}\cdot\text{mL}^{-1}$) | PF ^c | Reference ^d |
|---|-----------------|------|---|---|-----------------|------------------------|
| (1) poly(acrylamide) grafted onto cross-linked poly(4-vinyl pyridine) (P4-VP-g-PAm) | AFS | 1-8 | 4.1 | 2 | 20 | [9] |
| (2) Silica gel/2-thiophenecarboxaldehyde | AAS | 2 | 2 | 4.75 | 1000 | [10] |
| (3) Sodium dodecyl sulphate-coated magnetite nanoparticles/Michler's Thioketone complexes | ICP-AES | 3 | — | 40 | 1230 | [11] |
| (4) Magnetic nanoparticles doped with 1,5-diphenylcarbazine | CV-AAS | 6 | 0.22 | 160 | 100 | [12] |
| (5) Poly-allylthiourea | CV-AAS | 2 | 1.1 | 80 | 160 | [13] |
| (6) Silica gel/2-(2-oxoethyl)hydrazine | ICP-AES | 4 | 0.18 | 100 | 50 | [14] |
| (7) Polyaniline (PANI) | gold trap-CVAAS | 1-12 | 0.49 | 0.05 | 120 | [15] |
| (8) Hg(II)-Ionic imprinted polymers-thymine | AFS | 8 | 0.014 | 30 | 200 | [16] |
| (9) Silica gel/cysteine | CV-AAS | 1-7 | 0.69 | 1.5 | 40 | [17] |
| (10) Alumina/dimethylsulfoxide | AAS | 1-2 | 381 | — | 1000 | [18] |
| (11) C18/Isopropyl 2-[(isopropoxycarbothioly)disulfany]ethane thioate | CV-AAS | 3-7 | 0.015 | 5 | >150 | [19] |
| (12) Hg(II)-imprinted ion polymer | CV-AAS | 8 | 0.205 | 50 | 200 | [20] |
| (13) Agar powder modified with 2-mercaptobenzimidazole | CV-AAS | 2-3 | 1.89 | 20 | 100 | [21] |
| (14) Hg(II)-imprinted thiol-functionalized mesoporous sorbent | ICP-AES | 4-8 | 0.022 | 390 | 150 | [22] |
| (15) Silica gel immobilized 5-phenylazo-8-hydroxyquinoline | CV-AFS | 4 | 0.027 | 0.21 | >250 | This work |

^aDetection technique; ^blimit of detection; ^cpreconcentration factor; ^dreference.

Moreover, LOD achieved by CV-AFS is also low as compared to other reported techniques. Even though the adsorption capacity of the studied resin is considered low, it does not seem to restrict the objectives of the analytical technique developed, that is, recovery of trace levels of mercury. High adsorption capacities of resins are rather preferable for removal studies of mercury.

In summary, 5Ph8HQ has been widely used for the preconcentration of trace levels of metals. It has been proven to be robust and exhibiting excellent affinity towards transition elements. However, it has not been examined for the extraction of mercury. Therefore, in this study, we have reported the adsorption dynamics of mercury. Results have shown that it is totally absorbed by 5Ph8HQ within the first 30 minutes of contact time with $t_{1/2}$ 5 minutes, following Langmuir adsorption model. At pH 4, the affinity of mercury is unchallenged by other metals, except for Cu(II), which have shown higher K_d value. With these latter characteristics, 5Ph8HQ was examined for the preconcentration of trace levels of Hg(II). The developed method showed quantitative recoveries of Hg(II) with LOD = 0.21 pg mL⁻¹ and RSD = 3–6% using CV-AFS.

Acknowledgment

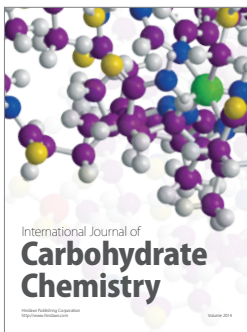
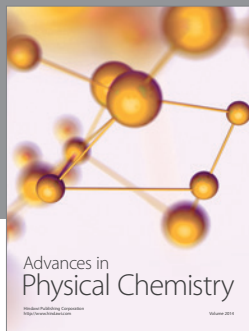
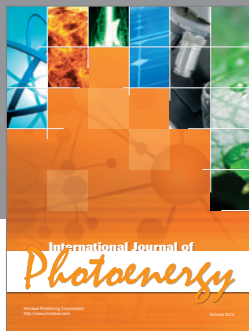
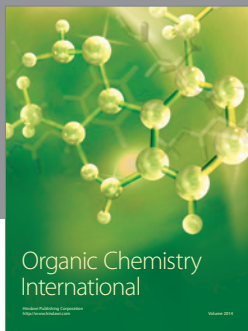
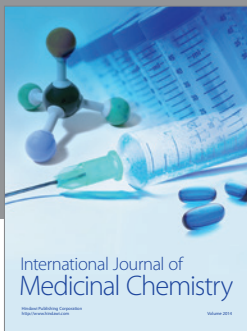
The authors would like to thank David Dumoulin, Romain Descamps (Université Lille 1), and Abdel Boughriet (Université d'Artois) for their technical assistance.

References

- [1] M. Tian, N. Song, D. Wang et al., "Applications of the binary mixture of sec-octylphenoxyacetic acid and 8-hydroxyquinoline to the extraction of rare earth elements," *Hydrometallurgy*, vol. 111-112, no. 1, pp. 109–113, 2012.
- [2] F. Malamas, M. Bengtsson, and G. Johansson, "On-line trace metal enrichment and matrix isolation in atomic absorption spectrometry by a column containing immobilized 8-quinolinol in a flow-injection system," *Analytica Chimica Acta*, vol. 160, pp. 1–10, 1984.
- [3] P. Y. T. Chow and F. F. Cantwell, "Calcium sorption by immobilized oxine and its use in determining free calcium ion concentration in aqueous solution," *Analytical Chemistry*, vol. 60, no. 15, pp. 1569–1573, 1988.
- [4] M. R. Weaver and J. M. Harris, "In situ fluorescence studies of aluminum ion complexation by 8-hydroxyquinoline covalently bound to silica," *Analytical Chemistry*, vol. 61, no. 9, pp. 1001–1010, 1989.
- [5] M. Howard, H. A. Jurbergs, and J. A. Holcombe, "Comparison of silica-immobilized poly(L-cysteine) and 8-hydroxyquinoline for trace metal extraction and recovery," *Journal of analytical atomic spectrometry*, vol. 14, no. 8, pp. 1209–1214, 1999.
- [6] S. Cerutti, M. F. Silva, J. A. Gásquez, R. A. Olsina, and L. D. Martinez, "On-line preconcentration/determination of cadmium in drinking water on activated carbon using 8-hydroxyquinoline in a flow injection system coupled to an inductively coupled plasma optical emission spectrometer," *Spectrochimica Acta B*, vol. 58, no. 1, pp. 43–50, 2003.
- [7] M. A. Marshall and H. A. Mottola, "Synthesis of silica-immobilized 8-quinolinol with (aminophenyl)trimethoxysilane," *Analytical Chemistry*, vol. 55, no. 13, pp. 2089–2093, 1983.
- [8] R. D. Shannon, "effective ionic radii and systematic studies of interatomic distances in halides and chalcogenides," *Acta Crystallographica A*, vol. 32, pp. 751–767, 1976.
- [9] O. Yayayürük, E. Henden, and N. Bıcak, "Determination of mercury(II) in the presence of methylmercury after preconcentration using poly(acrylamide) grafted onto cross-linked poly(4-vinyl pyridine): application to mercury speciation," *Analytical Sciences*, vol. 27, no. 8, pp. 833–838, 2011.
- [10] E. M. Soliman, M. B. Saleh, and S. A. Ahmed, "New solid phase extractors for selective separation and preconcentration of mercury (II) based on silica gel immobilized aliphatic amines 2-thiophenecarboxaldehyde Schiff's bases," *Analytica Chimica Acta*, vol. 523, no. 1, pp. 133–140, 2004.
- [11] M. Faraji, Y. Yamini, and M. Rezaee, "Extraction of trace amounts of mercury with sodium dodecyl sulphate-coated magnetite nanoparticles and its determination by flow injection inductively coupled plasma-optical emission spectrometry," *Talanta*, vol. 81, no. 3, pp. 831–836, 2010.
- [12] Y. Zhai, S. Duan, Q. He, X. Yang, and Q. Han, "Solid phase extraction and preconcentration of trace mercury(II) from aqueous solution using magnetic nanoparticles doped with 1,5-diphenylcarbazide," *Microchimica Acta*, vol. 169, no. 3, pp. 353–360, 2010.
- [13] W. Qu, Y. Zhai, S. Meng, Y. Fan, and Q. Zhao, "Selective solid phase extraction and preconcentration of trace mercury(II) with poly-allylthiourea packed columns," *Microchimica Acta*, vol. 163, no. 3-4, pp. 277–282, 2008.
- [14] X. Chai, X. Chang, Z. Hu, Q. He, Z. Tu, and Z. Li, "Solid phase extraction of trace Hg(II) on silica gel modified with 2-(2-oxoethyl)hydrazine carbothioamide and determination by ICP-AES," *Talanta*, vol. 82, no. 5, pp. 1791–1796, 2010.
- [15] M. V. B. Krishna, D. Karunasagar, S. V. Rao, and J. Arunachalam, "Preconcentration and speciation of inorganic and methyl mercury in waters using polyaniline and gold trap-CVAAS," *Talanta*, vol. 68, no. 2, pp. 329–335, 2005.
- [16] S. Xu, L. Chena, J. Li, Y. Guan, and H. Lu, "Novel Hg²⁺-imprinted polymers based on thymine-Hg²⁺-thymine interaction for highly selective preconcentration of Hg²⁺ in water samples," *Journal of Hazardous Materials*, vol. 237-238, pp. 347–354, 2012.
- [17] E. K. Mladenova, I. G. Dakova, D. L. Tsalev, and I. B. Karadjova, "Mercury determination and speciation analysis in surface waters," *Central European Journal of Chemistry*, vol. 10, pp. 1175–1182, 2012.
- [18] E. M. Soliman, M. B. Saleh, and S. A. Ahmed, "Alumina modified by dimethyl sulfoxide as a new selective solid phase extractor for separation and preconcentration of inorganic mercury(II)," *Talanta*, vol. 69, no. 1, pp. 55–60, 2006.
- [19] M. Shamsipur, A. Shokrollahi, H. Sharghi, and M. M. Eskandari, "Solid phase extraction and determination of sub-ppb levels of hazardous Hg²⁺ ions," *Journal of Hazardous Materials*, vol. 117, no. 2-3, pp. 129–133, 2005.
- [20] Y. Liu, X. Chang, D. Yang, Y. Guo, and S. Meng, "Highly selective determination of inorganic mercury(II) after preconcentration with Hg(II)-imprinted diazoaminobenzene-vinylpyridine copolymers," *Analytica Chimica Acta*, vol. 538, no. 1-2, pp. 85–91, 2005.
- [21] N. Pourreza and K. Ghanemi, "Determination of mercury in water and fish samples by cold vapor atomic absorption

- spectrometry after solid phase extraction on agar modified with 2-mercaptobenzimidazole," *Journal of Hazardous Materials*, vol. 161, no. 2-3, pp. 982-987, 2009.
- [22] Z. Fan, "Hg(II)-imprinted thiol-functionalized mesoporous sorbent micro-column preconcentration of trace mercury and determination by inductively coupled plasma optical emission spectrometry," *Talanta*, vol. 70, no. 5, pp. 1164-1169, 2006.
- [23] J. M. Hill, "Silica gel as an insoluble carrier for the preparation of selective chromatographic adsorbents. The preparation of 8-hydroxyquinoline substituted silica gel for the chelation chromatography of some trace metals," *Journal of Chromatography A*, vol. 76, no. 2, pp. 455-458, 1973.
- [24] M. A. Marshall and H. A. Mottola, "Performance studies under flow conditions of silica-immobilized 8-quinolinol and its application as a preconcentration tool in flow injection/atomic absorption determinations," *Analytical Chemistry*, vol. 57, no. 3, pp. 729-733, 1985.
- [25] J. R. Jezorek, K. H. Faltynski, L. G. Blackburn, P. J. Henderson, and H. D. Medina, "Silica-bound complexing agents: some aspects of synthesis, stability and pore size," *Talanta*, vol. 32, no. 8, pp. 763-770, 1985.
- [26] A. Goswami, A. K. Singh, and B. Venkataramani, "8-Hydroxyquinoline anchored to silica gel via new moderate size linker: synthesis and applications as a metal ion collector for their flame atomic absorption spectrometric determination," *Talanta*, vol. 60, pp. 1141-1154, 2003.
- [27] U. Pyell and G. Stork, "Preparation and properties of an 8-hydroxyquinoline silica gel, synthesized via mannich reaction," *Fresenius' Journal of Analytical Chemistry*, vol. 342, no. 4-5, pp. 281-286, 1992.
- [28] M. Lührmann, N. Stelter, and A. Ketrup, "Synthesis and properties of metal collecting phases with silica immobilized 8-Hydroxyquinoline," *Fresenius' Zeitschrift für Analytische Chemie*, vol. 322, no. 1, pp. 47-52, 1985.
- [29] V. A. Tertykh, V. V. Yanishpolskii, and O. Y. Panova, "Covalent attachment of some phenol derivatives to the silica surface by use of single-stage aminomethylation," *Journal of Thermal Analysis and Calorimetry*, vol. 62, no. 2, pp. 545-549, 2000.
- [30] Z. Wang, M. Jing, F. S. C. Lee, and X. Wang, "Synthesis of 8-hydroxyquinoline bonded silica (SHQ) and its application in flow injection inductively coupled plasma mass spectrometry analysis of trace metals in seawater," *Chinese Journal of Analytical Chemistry*, vol. 34, no. 4, pp. 459-463, 2006.
- [31] R. H. Uibel and J. M. Harris, "In situ raman spectroscopy studies of metal ion complexation by 8-hydroxyquinoline covalently bound to silica surfaces," *Analytical Chemistry*, vol. 74, no. 19, pp. 5112-5120, 2002.
- [32] R. H. Uibel and J. M. Harris, "Spectroscopic studies of proton-transfer and metal-ion binding of a solution-phase model for silica-immobilized 8-hydroxyquinoline," *Analytica Chimica Acta*, vol. 494, no. 1-2, pp. 105-123, 2003.
- [33] M. Hebrant, M. Rose-Helene, and A. Walcarius, "Metal ion removal by ultrafiltration of colloidal suspensions of organically modified silica," *Colloids and Surfaces A*, vol. 417, pp. 65-72, 2013.
- [34] K. F. Sugawara, H. H. Weetall, and G. D. Schucker, "Preparation, properties, and applications of 8-hydroxyquinoline immobilized chelate," *Analytical Chemistry*, vol. 46, no. 4, pp. 489-492, 1974.
- [35] R. E. Sturgeon, S. S. Berman, S. N. Willie, and J. A. H. Desauiniere, "Preconcentration of trace elements from seawater with silica-immobilized 8-hydroxyquinoline," *Analytical Chemistry*, vol. 53, no. 14, pp. 2337-2340, 1981.
- [36] J. W. McLaren, "Determination of trace metals in seawater by inductively coupled plasma mass spectrometry with preconcentration on silica-immobilized 8-hydroxyquinoline," *Analytical Chemistry*, vol. 57, no. 14, pp. 2907-2911, 1985.
- [37] B. K. Esser, A. Volpe, J. M. Kenneally, and D. K. Smith, "Preconcentration and purification of rare earth elements in natural waters using silica-immobilized 8-hydroxyquinoline and a supported organophosphorus extractant," *Analytical Chemistry*, vol. 66, no. 10, pp. 1736-1742, 1994.
- [38] S. M. Nelms, G. M. Greenway, and R. C. Hutton, "Application of multi-element time-resolved analysis to a rapid on-line matrix separation system for inductively coupled plasma mass spectrometry," *Journal of Analytical Atomic Spectrometry*, vol. 10, no. 11, pp. 929-933, 1995.
- [39] B. L. Rivas, B. Urbano, S. A. Pooley, I. Bustos, and N. Escalona, "Mercury and lead sorption properties of poly(ethyleneimine) coated onto silica gel," *Polymer Bulletin*, vol. 68, pp. 1577-1588, 2012.
- [40] S. Lagergren, "Zur theorie der sogenannten adsorption gelöster stoffe," *Kungliga Svenska Vetenskapsakademiens Handlingar*, vol. 24, no. 4, pp. 1-39, 1898.
- [41] Y. S. Ho and G. McKay, "Pseudo-second order model for sorption processes," *Process Biochemistry*, vol. 34, no. 5, pp. 451-465, 1999.
- [42] W. J. Weber and J. C. Morris, "Kinetics of adsorption on carbon from solution," *Journal of the Sanitary Engineering Division*, vol. 89, no. 2, pp. 31-60, 1963.
- [43] H. Freundlich, "Ueber die adsorption in lösungen," *Zeitschrift für Physikalische Chemie*, vol. 57, pp. 385-470, 1907.
- [44] H. Dikici and K. Salti, "Equilibrium and kinetics characteristics of copper(II) sorption into gytiya," *Bulletin of Environmental Contamination and Toxicology*, vol. 84, pp. 147-151, 2010.
- [45] M. M. Dubinin and L. V. Raudushkevich, "Equation of the characteristics curve of activated charcoal," *Proceedings of the Academy of Sciences Physical Chemistry Section, USSR*, vol. 55, pp. 331-333, 1947.
- [46] M. L. Ferreira and M. E. Gschaider, "Theoretical and experimental study of Pb²⁺ and Hg²⁺ adsorption on biopolymers. 1: theoretical study," *Macromolecular Bioscience*, vol. 1, no. 6, pp. 233-248, 2001.
- [47] A. W. Adamson, *Physical Chemistry of Surfaces*, Wiley, New York, NY, USA, 5th edition, 1990.
- [48] A. E. Martell and L. G. Sillen, *Stability Constants of Metal Ion Complexes*, Chemical Society, London, UK, 2nd edition, 1964.
- [49] D. R. Turner, M. Whitfield, and A. G. Dickson, "The equilibrium speciation of dissolved components in freshwater and sea water at 25°C and 1 atm pressure," *Geochimica et Cosmochimica Acta*, vol. 45, no. 6, pp. 855-881, 1981.
- [50] W. T. Rees, "Fluorimetric determination of very small amounts of aluminium," *The Analyst*, vol. 87, no. 1032, pp. 202-206, 1962.
- [51] K.-L. Yang, S.-J. Jiang, and T.-J. Hwang, "Determination of titanium and vanadium in water samples by inductively coupled plasma mass spectrometry with on-line preconcentration," *Journal of Analytical Atomic Spectrometry*, vol. 11, no. 2, pp. 139-143, 1996.
- [52] J. R. Dojlido and G. A. Best, *Chemistry of Water and Water Pollution*, Ellis Horwood Series in Water and Wastewater Technology, Ellis Horwood, New York, NY, USA, 1993.

- [53] A. Denizli, K. Kesenci, Y. Arica, and E. Pişkin, "Dithiocarbamate-incorporated monosize polystyrene microspheres for selective removal of mercury ions," *Reactive and Functional Polymers*, vol. 44, no. 3, pp. 235–243, 2000.
- [54] P. Stathi, K. Dimos, M. A. Karakassides, and Y. Deligiannakis, "Mechanism of heavy metal uptake by a hybrid MCM-41 material: surface complexation and EPR spectroscopic study," *Journal of Colloid and Interface Science*, vol. 343, no. 1, pp. 374–380, 2010.
- [55] V. C. Taty-Costodes, H. Fauduet, C. Porte, and A. Delacroix, "Removal of Cd(II) and Pb(II) ions, from aqueous solutions, by adsorption onto sawdust of *Pinus sylvestris*," *Journal of Hazardous Materials*, vol. 105, no. 1–3, pp. 121–142, 2003.
- [56] M. V. Dinu and E. S. Dragan, "Evaluation of Cu²⁺, Co²⁺ and Ni²⁺ ions removal from aqueous solution using a novel chitosan/clinoptilolite composite: kinetics and isotherms," *Chemical Engineering Journal*, vol. 160, no. 1, pp. 157–163, 2010.
- [57] M. Mureseanu, A. Reiss, I. Stefanescu et al., "Modified SBA-15 mesoporous silica for heavy metal ions remediation," *Chemosphere*, vol. 73, no. 9, pp. 1499–1504, 2008.
- [58] A. Sayari, S. Hamoudi, and Y. Yang, "Applications of pore-expanded mesoporous silica. 1. Removal of heavy metal cations and organic pollutants from wastewater," *Chemistry of Materials*, vol. 17, no. 1, pp. 212–216, 2005.
- [59] H. Irving and R. J. P. Williams, "Order of stability of metal complexes," *Nature*, vol. 162, no. 4123, pp. 746–747, 1948.
- [60] A. Benhamou, M. Baudu, Z. Derriche, and J. P. Basly, "Aqueous heavy metals removal on amine-functionalized Si-MCM-41 and Si-MCM-48," *Journal of Hazardous Materials*, vol. 171, no. 1–3, pp. 1001–1008, 2009.
- [61] N. Ünlü and M. Ersoz, "Adsorption characteristics of heavy metal ions onto a low cost biopolymeric sorbent from aqueous solutions," *Journal of Hazardous Materials*, vol. 136, no. 2, pp. 272–280, 2006.
- [62] L. Wang, R. Xing, S. Liu et al., "Synthesis and evaluation of a thiourea-modified chitosan derivative applied for adsorption of Hg(II) from synthetic wastewater," *International Journal of Biological Macromolecules*, vol. 46, no. 5, pp. 524–528, 2010.
- [63] O. Hakami, Y. Zhang, and C. J. Banks, "Thiol-functionalized mesoporous silica-coated magnetite nanoparticles for high efficiency removal and recovery of Hg from water," *Water Research*, vol. 46, pp. 3913–3922, 2012.
- [64] L. Bai, H. Hu, W. Fu et al., "Synthesis of a novel silica-supported dithiocarbamate adsorbent and its properties for the removal of heavy metal ions," *Journal of Hazardous Materials*, vol. 195, pp. 261–275, 2011.
- [65] L. Qi and Z. Xu, "Lead sorption from aqueous solutions on chitosan nanoparticles," *Colloids and Surfaces A*, vol. 251, no. 1–3, pp. 183–190, 2004.
- [66] S. N. Willie, H. Tekgul, and R. E. Sturgeon, "Immobilization of 8-hydroxyquinoline onto silicone tubing for the determination of trace elements in seawater using flow injection ICP-MS," *Talanta*, vol. 47, no. 2, pp. 439–445, 1998.
- [67] H. Watanabe, K. Goto, S. Taguchi, J. W. McLaren, S. S. Berman, and D. S. Russell, "Preconcentration of trace elements in seawater by complexation with 8-hydroxyquinoline and adsorption on C18 bonded silica gel," *Analytical Chemistry*, vol. 53, no. 4, pp. 738–739, 1981.
- [68] G. L. Long and J. D. Winefordner, "Limit of detection: a closer look at the IUPAC definition," *Analytical Chemistry*, vol. 55, no. 7, pp. 712–724, 1983.



Hindawi

Submit your manuscripts at
<http://www.hindawi.com>

